Proc. of the 30th International Slovak–Polish Scientific Conference on Machine Modelling and Simulations 2025

Research Test Rig for the Analysis of Physical Phenomena Related to the Tension Force of Transport Straps

M. Szulc[a,*], D. Wilczyński[b], D. Wojtkowiak[b] and K. Talaśka[b]

[a] *MSprojekt plus Sp. z o.o., J.H. Dąbrowskiego 26a, 64-330 Opalenica, Poland*
[b] *Faculty of Mechanical Engineering, Institute of Machine Design, Poznan University of Technology, Piotrowo 3, 61-138 Poznań, Poland*

Doi: 10.12693/APhysPolA.149.S49 *e-mail: m.szulc@msprojektplus.pl

The paper presents the development of a physical research test rig dedicated to the analysis of physical phenomena related to the tension force in transport straps used for cargo securing. The proposed design provides a physical representation of forces acting on the straps and enables the investigation of physical interactions that occur under real transport conditions. By allowing controlled variation of belt angles, load distribution, and the physical position of the centre of gravity, the rig makes it possible to reproduce and examine physical phenomena that critically affect strap tension and cargo stability. The study emphasises the importance of analysing these physical processes in order to better understand the mechanisms of force transmission and the physical behaviour of securing systems. A detailed description of the test rig's construction, its physical operating principle, and its functional features is provided. Furthermore, a structural strength evaluation was performed using the finite element method, and the obtained results from physical experiments are discussed. The findings provide an in-depth insight into the physical mechanisms governing strap tension and may serve as a valuable reference for both designers and practitioners concerned with the physical conditions of transport safety.

topics: transport belts, tensioning of transport belts, belt tension testing, tension force

1. Introduction

Freight transport is expanding alongside the growth of trade, which in turn is driven by increasing human needs. The demand for various types of products is rising year by year, and the ease of access to these goods, combined with relatively low prices, makes it easier for consumers to decide to purchase them. However, few of us are aware of how many kilometres an item we order must travel to reach us. Depending on the place of production, transport may be carried out by sea, air, or land. Regardless of the method, appropriate load securing systems must be used. Improperly secured cargo can loosen, resulting in shifting during transport, which directly affects the stability of the vehicle. This can lead to accidents that put human health and lives at risk. There are many examples of such accidents, yet relatively few effective methods exist to counteract the loosening of load restraints [1–3]. The most commonly used method for securing loads is lashing straps, and in road transport, where accidents involving people are most frequent, transport belts are predominantly used. Research into the behaviour of lashing systems during transport can help identify solutions to prevent cargo shifting and reduce the number of accidents. The tension force in transport belts during transit is influenced by many factors, including: dynamic forces caused by acceleration, braking, and cornering; road surface conditions (vibrations, unevenness); cargo settlement and shifting; and environmental conditions such as temperature and humidity, which affect belt materials [4–8]. Continuous monitoring of belt tension is crucial for safe and efficient cargo transport. The implementation of automated tension monitoring systems significantly reduces the risk of cargo displacement and securing failures [9]. The future development of intelligent load securing technologies will further enhance transport safety and operational efficiency in the logistics sector. The application of real-time belt tension monitoring systems offers numerous advantages: improved cargo safety and transport reliability, reduced need for manual tension checks during transit, early detection of belt loosening or failure, better compliance with cargo securing regulations, and lower operating costs through prevention of excessive belt wear [10–12]. In paper [13], the applicability of tension sensors sewn into the belt structure was investigated. It was demonstrated that such sensors can measure and monitor belt tension during transport.

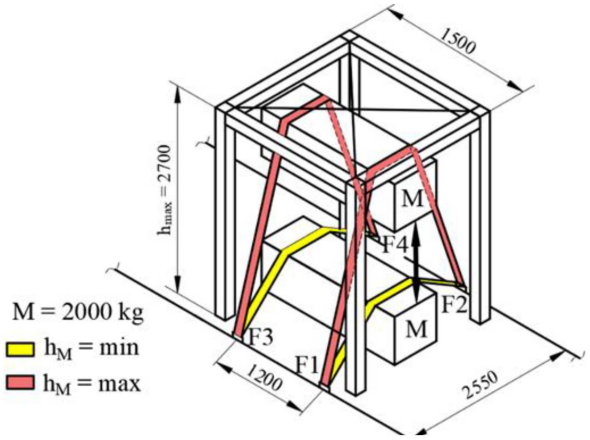

Fig. 1. General layout of the test setup with defined measurement points.

Fig. 2. General view of the UP-01-4P measuring device.

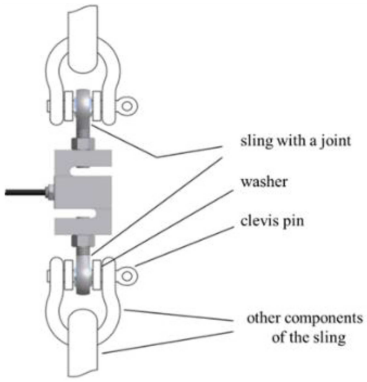

Fig. 3. General view of the force sensor mounted inline with the belt tension.

2. Methods and materials

2.1. Purpose of the test stand construction

The purpose of constructing the test stand is to identify the cause of loosening in securing lashings by conducting a series of simulations of cargo being transported under real-world conditions. Gathering as much information as possible about the forces involved, their characteristics, and critical stresses at the attachment points will allow for the determination of tension limits within which the cargo remains safely secured. The test stand is designed to replicate various types of cargo placed on the load bed of a truck.

The testing itself will be carried out on public roads, within regular traffic, along a defined route. All research activities will be conducted in accordance with the PN-EN 12195-2 standard, which pertains to cargo securing methods.

2.2. Design assumptions

In the design process of the aforementioned test stand, it was assumed that the structure would be made of steel profiles. The stand is intended to have the form of a cage that fits on the cargo bed of a vehicle, with four contact points connected to the floor plate (Fig. 1).

The width of the cage should allow for the installation of two transport belts securing the simulated cargo in two planes. The mass core of the cargo is to be positioned centrally along the longitudinal axis of the vehicle, with the possibility of adjusting the height of its centre of gravity. The stand must allow for an increase in the core mass, depending on the research requirements. The baseline cargo mass is assumed to be 2000 kg (Fig. 1). The structure should allow for quick and easy adjustment of settings. To minimise the number of tools needed for calibration, one type of bolted connection should be used wherever possible. The design must also allow the stand to be safely, easily, and quickly loaded onto the cargo bed using standard material handling equipment (e.g., forklift truck).

2.3. Measuring device

To record the force values at the designated measurement points, the "UP-01-4P" device was used. It was specifically designed and manufactured for the purposes of this study. The device consists of four AXIS FB20k force sensors, an acceleration sensor, a temperature sensor, an SD card reader, and a central computer. All sensor values are recorded with a sampling interval of 1 ms. The device is powered by a 12 V supply drawn from the vehicle's electrical system. A voltage stabilisation unit is integrated into the system. The synchronised data logging system records all sensor values simultaneously and is automatically activated upon connection to the

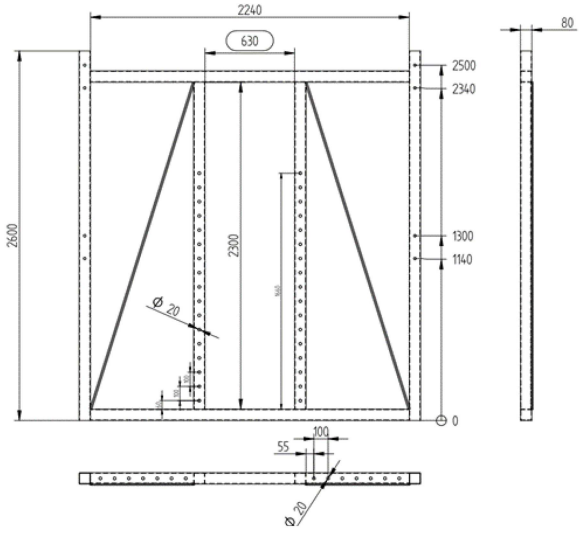

Fig. 4. Diagram of the main frame of the device base.

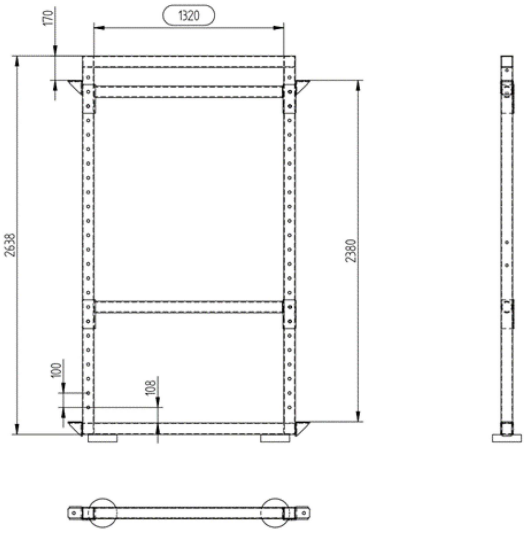

Fig. 5. Diagram of the adjustable frame of the device.

power source. It is crucial that the force sensors are not subjected to any external forces, such as those resulting from the self-weight of mounting hardware or strap tension at the moment the power is turned on. Figure 2 shows the UP-01-4P measurement device, while Fig. 3 presents the method of mounting the force sensor inline with the belt tension.

2.4. Design of the test stand

The design of the test stand structure was created in Solid Edge 2020 as a 3D solid model. The main, fixed frame is made from square profiles measuring $80\times80\times5$ mm^3, featuring laser-cut adjustment holes that allow for various centre of gravity settings and simulation of different cargo widths. The external dimensions are shown in Fig. 4.

The adjustable frames are made from square profiles measuring $80 \times 80 \times 5$ mm^3 with laser-cut adjustment holes used to change the cargo height. Once bolted to the main frame, the adjustable frames form a stable frame structure. The dimensions of the adjustable frame are shown in Fig. 5.

The support beams serve to hold the mass core (green colour in Fig. 6). Adjustment holes in the main frame allow for changing the height of the mass core in 100 mm increments. The corner beams of the load (Fig. 6, colour yellow) simulate strapped edges, and their height can be adjusted in 100 mm increments. The load width can be modified by shifting the adjustable frames relative to the fixed frame. These adjustments can also be made in 100 mm steps. Figure 6 shows the 3D model of the complete test device assembly. Figures 7 and 8 illustrate the range of securing transport belts on the device and the maximum adjustment ranges of the device setup.

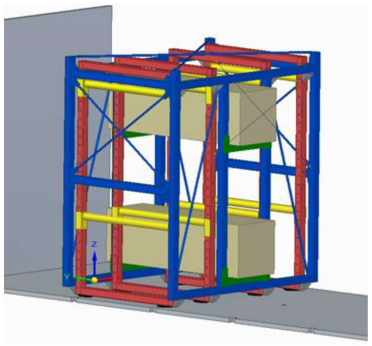

Fig. 6. General view of the 3D model of the complete device assembly.

2.5. FEM analysis of the structure

Finite element method (FEM) studies were conducted using Inventor software. Figures 9 and 10 present the analysis results related to displacements and stresses in the structure under a load applied at two points, each with a force of 25 kN. This corresponds to an unfavourable loading case with forces acting at the middle of the beams. All nodes and the device structure itself remained within the allowable strength limits. The design was positively approved.

2.6. Construction of the test stand

The structure of the designed test stand was manufactured by MSprojekt Maciej Szulc in accordance with the EXC2 standard. Subsequently, a

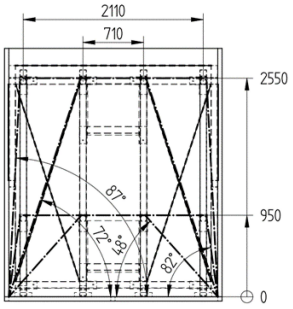

Fig. 7. General view of a range of securing transport belts on the device.

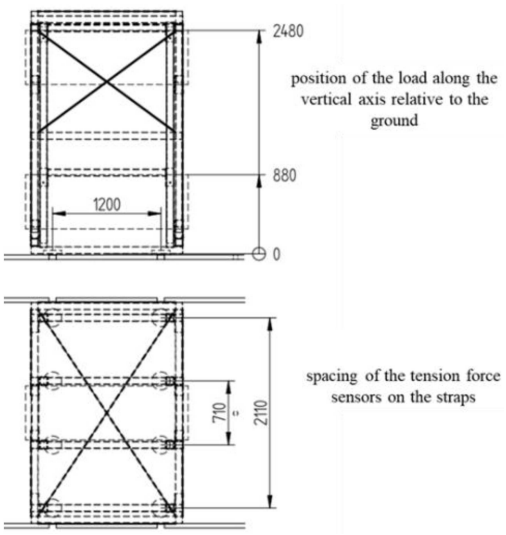

Fig. 8. Maximum adjustment ranges of the device.

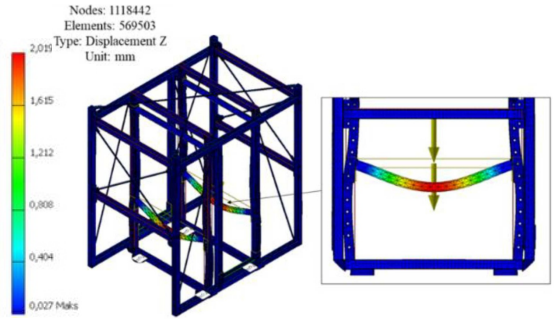

Fig. 9. FEM analysis — displacements.

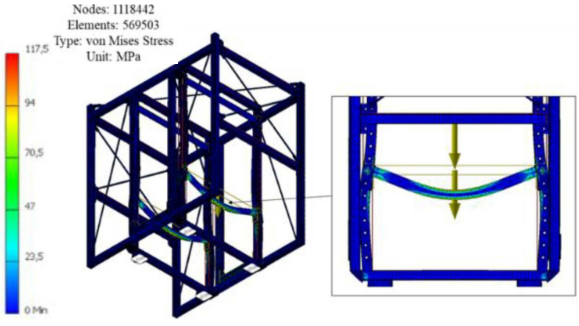

Fig. 10. FEM analysis — stresses.

Fig. 11. General view of the test stand mounted on the vehicle.

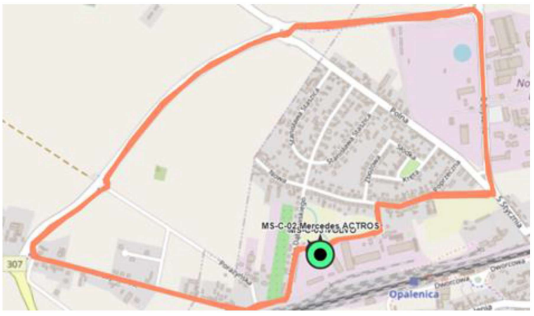

Fig. 12. General view of the GPS map of the vehicle's route segment.

zinc coating was applied to prevent corrosion of the steel parts, and the components were additionally powder-coated in different colours. The fixed frame is painted black, the adjustable frames are red, and the support elements and load corners are yellow (Fig. 11).

2.7. Test experiments with the assembled test stand

The tests were conducted in four configurations of the centre of gravity settings and the angles of attack of the transport straps. For one configuration, the test was repeated five times. Each repetition consisted of traversing the same route three times, which included sections of urban asphalt road, municipal asphalt road, a short segment made of concrete road slabs, and a gravel road with many potholes. One lap covered a distance of 5 km, completed in 7–8 min depending on traffic conditions. The tests were performed using a Mercedes Actros 1846 vehicle with a maximum gross weight of 12 tons. It is a two-axle vehicle with pneumatic suspension, equipped with a cargo-type load box measuring $7.5 \times 2.5 \times 2.8$ m^3.

TABLE I

Sample test results A1_B1-2.

A1_B1-2	t_s [s]	Pas1aF1 [N]	Pas1bF2 [N]	dif_1 [N]
1501	152.7	3949.8	4434.9	−485.02
7001	712.2	4467.1	5572.7	−1105.6
12501	1271.7	4477.1	5304.5	−827.4
18001	1831.1	4437.1	5551.1	−1113.9

TABLE II

Sample test results A1_B1-2 cont.

A1_B1-2	t_s [s]	Pas2aF3 [N]	Pas2bF4 [N]	dif_2 [N]
1501	152.7	4653.4	4545.7	107.8
7001	712.2	4594.9	4367.5	227.5
12501	1271.7	4504.7	4417.7	87.0
18001	1831.1	4551.6	4235.9	315.7

Figure 12 shows a photo of the GPS map of the vehicle's route segment. Figure 11 presents the test stand mounted on the vehicle. One test consisted of repeating the route shown in Fig. 12 three times, with approximately one-minute breaks between repetitions.

3. Results and discussion

The test results were processed using proprietary scripts created in the Spyder Python 3.12 environment with the pandas, numpy, and matplotlib libraries. The scripts were designed to compile the force values from four load cells (Pas1aF1, Pas1bF2, Pas2aF3, Pas2bF4; F_1, F_2, F_3, F_4) at four stopping points:

1 — before starting the journey,
2–3 — between the runs,
4 — after completing the drive (1501, 7001, 12501, 18001)

(see Tables I and II, where, as in Fig. 1: t_s — time intervals for recording force values, Pas1aF1 — force on strap no. 1 read from force sensor no. 1, Pas1bF2 — force on strap no. 1 read from force sensor no. 2, dif_1 — the difference in the read force value at ends 1 and 2 of strap no. 1, Pas2aF3 — force on strap no. 2 read from force sensor no. 3, Pas2bF4 — force on strap no. 2 read from force sensor no. 4, dif_2 — the difference in the read force value at ends 3 and 4 of strap no. 2, see Fig. 1).

The time stamps for each stopping point vary for each test, as the time taken to complete the route differed due to traffic conditions. This allows comparison of force values by observing the range of changes between them. Figure 13 shows the force

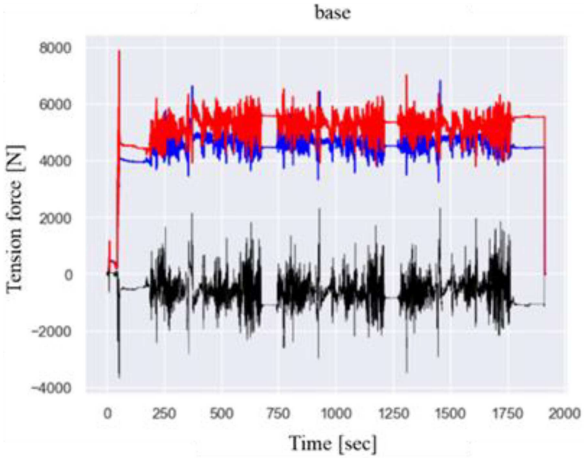

Fig. 13. Characteristics of changes in strap tension force values during the drive; values for strap no. 1: red colour — Pas1bF2, blue colour — Pas1aF1, black colour — difference in values (numbering according to Fig. 1).

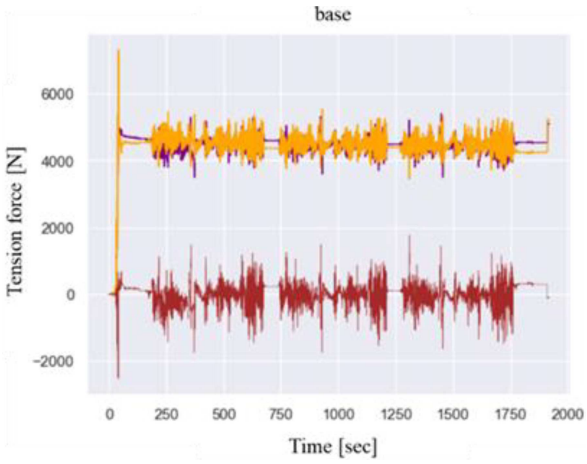

Fig. 14. Characteristics of changes in strap tension force values during the drive; values for strap no. 2: purple colour — Pas2bF4, yellow colour — Pas2aF, brown colour — difference in values (numbering according to Fig. 1).

values F_2 (red) and F_1 (blue), with the black line indicating the difference between forces F_1 and F_2. The initial pre-tension values, i.e., $F_1 = 3949.8$ N and $F_2 = 4434.9$ N (see Tables I and II), illustrate how significant the initial tension difference already is. This difference arises from the friction forces acting on the strapped cargo and amounts to 485.02 N (see Tables I and II). The theoretical assumptions predicted a decrease in this difference with each run and a reduction in the sum of the tension forces F_1 and F_2. However, the test revealed not only an increase in the tension difference between these forces up to 1113.9 N but also a 16% increase in the total strap tension force from 8384.7 to 9988.2 N. This indicates that the cargo shifted relative to the load

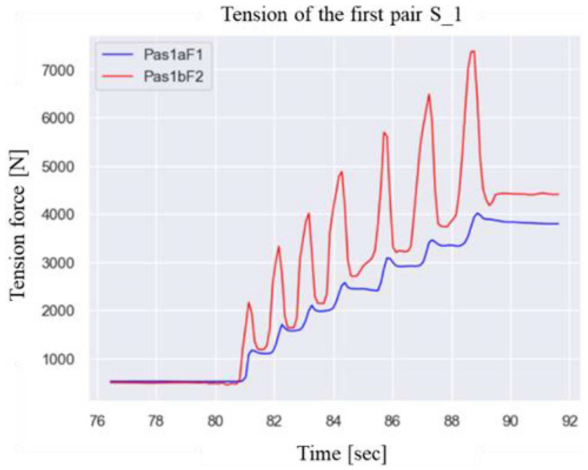

Fig. 15. Characteristics of changes in tension force of strap no. 1 during manual use of the buckle.

box, which is undesirable during transport. The values for strap no. 2 (Fig. 14) show a decrease in tension, as expected, by 3.4%. Factors influencing cargo behaviour include mainly the characteristics of the route, traffic intensity, and driving dynamics. The tests were conducted at consistent times of day by the same driver. The force difference graph for strap no. 1 during test A1_B1-2 presents several characteristic points on the route: curves, roundabouts, speed bumps, stops, and starts. The point with the greatest difference exceeding 4000 N is at the junction with the city bypass, where a 90° left turn must be immediately followed by a 90° right turn at $\approx$ 40 km/h. Such manoeuvrers change the direction of centrifugal forces, affecting the cargo's behaviour. Tests were carried out for four test stand settings, each repeated five times. The results are still under analysis. The labels correspond to those in Fig. 1.

Figure 15 shows a graphical chart of the increase in forces F_1 and F_2 for strap no. 1 during tensioning. The characteristic spikes in force F_2 correspond to the clicks of the transport strap tensioner buckle.

4. Conclusions

The tests were conducted correctly and successfully, and the results have been submitted for analysis. As an improvement, the measurement system should be additionally equipped with a power system switch accessible directly after sliding back the cargo box tarp. The electrical cables must also be protected to prevent mechanical damage. Adjusting the device settings is currently difficult and requires a three-person team and a forklift. It is necessary to remove the device from the cargo box. Rescaling the device takes $\approx$ 45 min. In future tests, the initial tension value of the transport straps should be established. From the analysis of the results, it can be concluded that the load shifted, as indicated by the increase in the sum of tension forces in strap no. 1. It is worth considering the possibility of monitoring the load displacement relative to the cargo box or mechanically securing the test rig by using cargo space partitions. For development purposes, it is also valuable to monitor the acceleration values of the test rig. These results may be helpful in the construction of a stationary test rig.

References

[1] W. Schlobohm, *Mocuj Ładunki ale prawidłowo! — Poradnik praktyczny*, CSK Transport–Logistyka–Doradztwo, Szczecin 2007.

[2] T. Skrucany, F. Synak, S. Semanova, J. Ondrus, V. Rievaj, in: *2018 XI Int. Science–Technical Conf. Automotive Safety*, IEEE, 2018.

[3] K. Kural, M. Voskuijl, T. Fengnian, J. Pauwelussen, *Transport* **29**, 363 (2014).

[4] European Commission, *European Best Practice Guidelines on Cargo Securing for Road Transport*, 2014 (accessed Aug 2025).

[5] European Committee for Standardization, EN 12195-1:2010, "Load restraint assemblies on road vehicles — Safety — Part 1: Calculation of lashing forces", CEN, Brussels 2010.

[6] VDI 2700, "Securing of Loads on Road Vehicles", Verein Deutscher Ingenieure, Düsseldorf 2014.

[7] Federal Motor Carrier Safety Administration, "Cargo Securement Rules", Part 393 Subpart I, 2014 (accessed Aug 2025).

[8] ISO 27956:2009, "Road vehicles — Securing of cargo in delivery vans — Requirements and test methods", International Organization for Standardization, Geneva 2009.

[9] T. Schlechter, J. Fischer, M. Röhrig, in: *2020 21st Int. Conf. on Research and Education in Mechatronics (REM 2020)*, IEEE, 2020.

[10] N. Dolzhenko, G. Imasheva, A. Berkesheva, O. Garmash, T. Beketov, *Transp. Res. J.* **10**, 105 (2021).

[11] Loadlok Systems, Cargo Securing Solutions and Tension Monitoring Devices, 2023 (accessed Aug 2025).

[12] SpanSet, Load Control Equipment and Dynamic Tension Monitoring Technologies, Manufacturer Brochure, 2023 (accessed Aug 2025).

[13] N. Lesser, B. Sadlovsky, *Acta Tech. Jaurinensis* **17**, 91 (2024).